Available online at www.sciencedirect.com
ScienceDirect
Journal of Pharmaceutical and Biomedical Analysis 44 (2007) 845–852
JOURNAL OF PHARMACEUTICAL AND BIOMEDICAL ANALYSIS
www.elsevier.com/locate/jpba

The application of microbore UPLC/oa-TOF-MS and ^{1}H NMR spectroscopy to the metabonomic analysis of rat urine following the intravenous administration of pravastatin

E.M. Lenz[a,*], R.E. Williams[a], J. Sidaway[b], B.W. Smith[c], R.S. Plumb[c], K.A. Johnson[c], P. Rainville[c], J. Shockcor[c], C.L. Stumpf[c], J.H. Granger[c], I.D. Wilson[a]

[a] *Department of Drug Metabolism and Pharmacokinetics, AstraZeneca, Mereside, Alderley Park, Macclesfield, Cheshire SK10 4TG, UK*
[b] *Global Safety Assessment, AstraZeneca, Mereside, Alderley Park, Macclesfield, Cheshire SK10 4TG, UK*
[c] *Waters Corporation, Milford, MA, USA*

Received 7 February 2007; received in revised form 26 April 2007; accepted 27 April 2007
Available online 3 May 2007

Abstract

The metabonomic effects of hepatotoxic doses of pravastatin on the urinary metabolic profiles of female rats have been investigated using ultra performance liquid chromatography (UPLC)–oa-TOF-MS and, independently, by ^{1}H NMR spectroscopy. UPLC was performed using a 1 mm microbore column packed with 1.7 μm particles. Examination of the data obtained from the individual animals, aided by statistical interpretation of the data, made it possible to identify potential markers for toxicological effects, with both NMR and UPLC–MS analysis highlighting distinct changes in the urinary metabolite profiles. These markers, which included elevated taurine and creatine, as well as bile acids, were consistent with hepatotoxicity in some animals, and this hypothesis was supported by histopathological and clinical chemistry findings. The analytical data from both techniques could be used to define a metabolic "trajectory" as toxicity developed and to provide an explanation for the lack of hepatotoxicity for one of the animals. The two analytical approaches (UPLC–MS and NMR) were found to be complementary whilst the use of a 1 mm i.d. × 100 mm column reduced the amount of sample required for analysis to 2 μL, compared with 10 μL for a 2.1 mm i.d. × 100 mm column. The 1 mm i.d. column also provided increased signal-to-noise without loss of chromatographic efficiency.

Keywords: LC–MS; ^{1}H NMR spectroscopy; Metabonomics; UPLC; TOF-MS; Microbore columns; Pravastatin; Biomarkers; Hepatotoxicity

1. Introduction

Metabonomics is a term applied to the global metabolite profiling of biological samples, particularly biofluids such as urine and plasma, combined with multivariate statistical analysis in order to determine changes in response to, e.g. a toxic insult, disease or genetic modification [1,2]. One area of considerable interest for the application of this approach is in the investigation and monitoring of xenobiotic toxicity (particularly drugs) as part of the safety evaluation process. In this type of study both markers of toxicity and a mechanistic understanding are sought. The potential of metabonomics in this area is well recognised [3] and there have already been initiatives to build metabonomic databases that aim to characterise the effects of typical, well known toxins, and to further investigate the underlying mechanisms [4]. More recently studies have shown that it may in fact be possible to use metabonomics techniques to predict toxicity based on pre-dose samples (pharmacometabonomics) [5].

In this type of analysis the aim is to discover potential biomarkers and by definition these are not defined prior to the analysis. It is therefore important to obtain as wide as possible coverage of the metabolome and to this end a variety of analytical technologies are currently being used to generate profiles. These include high field proton NMR spectroscopy [6], GC–MS and GC × GC–MS [7–9], HPLC/UPLC–MS [10–13], and CE–MS [14,15] (for a recent review of analytical methodology see Ref. [16]). We have previously demonstrated in a number of studies that HPLC–MS and ^{1}H NMR spectroscopy provide complementary data (e.g. [17–19]) and, when these techniques are combined together for the analysis of the same samples, they give a much

* Corresponding author. Tel.: +44 1625 514653; fax: +44 1625 516962.
E-mail address: Eva.Lenz@astrazeneca.com (E.M. Lenz).

0731-7085/$ – see front matter © 2007 Elsevier B.V. All rights reserved.
doi:10.1016/j.jpba.2007.04.035

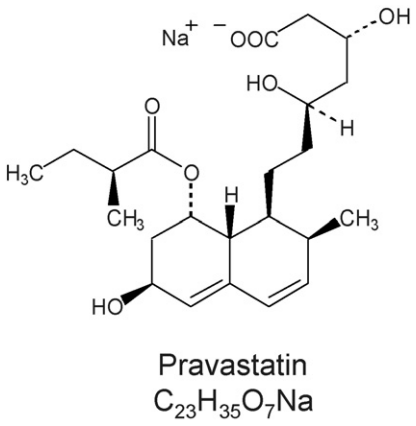

Fig. 1. The structure of pravastatin (sodium salt).

more comprehensive view of the effects of a particular treatment or disease state (e.g. see Ref. [20] for the application of UPLC–MS, GC–MS and ^{1}H NMR spectroscopy to the metabonomic analysis of rat plasma). As we have shown elsewhere, both HPLC–MS and UPLC–MS are proving to be valuable additions to the techniques available for metabonomic analysis [12,21,22]. In particular the introduction of UPLC, based on the use of sub 2 μm particles and 2.1 mm i.d. narrow bore columns, is proving to be of benefit. Thus UPLC, because it provides higher chromatographic resolution than HPLC, can either be used to give a much increased peak capacity for the equivalent analysis time [12,21], or a greatly increased throughput with the detection of a similar number of components [22].

Here ^{1}H NMR spectroscopy and UPLC–MS, employing a microbore (1 mm i.d.) column, are applied for the metabonomic analysis of rat urine following the continuous infusion of pravastatin, a cholesterol-lowering drug (structure in Fig. 1) that inhibits HMG-CoA reductase, the rate-limiting enzyme of cholesterol synthesis. A comparison with UPLC on an equivalent narrow bore (2.1 mm i.d.) column was also performed. The dose employed was designed to explore the toxicological properties of the compound and derive characteristic biomarkers.

2. Experimental

2.1. Chemicals

Acetonitrile (HPLC grade) was purchased from JT Baker (NJ, USA), ammonium formate and formic acid (spectroscopic grade) was purchased from Sigma/Aldrich (MO, USA). Distilled water was purified "in-house" using a MilliQ system Millipore (MA, USA). Leucine enkephalin was obtained from Sigma–Aldrich (MO, USA). Pravastatin (sodium salt, Fig. 1), batch 200107010 was supplied by South China Pharmachem International Ltd., and had a purity of greater than 99%.

2.2. Animal studies

Four female rats (13–15 weeks old) Wistar Han: substrain Crl:WI(Glx/BRL/Han) IGSBR were fitted with an indwelling catheter (entering via a tail vein), for intravenous administration by continuous infusion, emptying into the thoracic *vena cava*. Sterile physiological saline was continuously infused through the cannula at a rate of between 0.5 and 1 mL/kg/h, for at least 6 days, to allow the animal to recover from surgery. Following recovery, either infusion of vehicle (sterile physiological saline) or pravastatin (10 mg/mL in sterile physiological saline) commenced at an infusion rate of 2 mL/kg/h, corresponding to 500 mg/kg/day. Pravastatin was administered to three animals whilst the fourth animal was used as a control and was dosed with vehicle only.

The animals were housed in polypropylene cages and were allowed free access to food and water throughout the experiment. Urine samples were collected on the day prior to dosing (day −1) and days 1, 2, 3 and 4 following the commencement of dosing. Individual 18 h urine collections were taken commencing at about 15:00 h and finishing at about 09:00 h the next day. Samples were stored frozen at −20 °C prior to analysis.

At the termination of the study a blood sample was obtained from each animal for clinical chemistry and a small sample of the left lateral liver lobe, preserved in neutral buffered formalin, was also taken.

3. Sample analysis

3.1. Histopathology and clinical chemistry

Histological sections were prepared, stained with haematoxylin and eosin, and examined by light microscopy. Plasma levels of alkaline phosphatase, alanine aminotransferase, aspartate aminotransferase, glucose, cholesterol and triglycerides were determined using standard colorimetric assays.

3.2. Chromatography

For UPLC–MS the samples were diluted 1:5 (20 μL sample plus 80 μL of distilled water) and transferred to a total recovery auto-sampler vial for analysis.

Chromatographic separations were performed on either a 1 or 2.1 mm i.d. × 100 mm ACQUITY^{TM} 1.7 μm column (Waters Corp., Milford, USA) using an ACQUITY^{TM} UPLC system. Columns were maintained at 40 °C and eluted with a linear gradient of 0–95% B, where A = water with 0.1% formic acid and B = acetonitrile with 0.1% formic acid. The gradient duration was 30 min at a flow rate of 136 μL/min (1 mm i.d.) or 500 μL/min (2.1 mm i.d.) with a 2 min recycle time. Either 2 or 10 μL aliquots of sample were loaded onto the 1 and 2.1 mm i.d. columns, respectively. The column eluent was analysed by time of flight mass spectrometry using positive ion electrospray ionisation (ESI).

3.3. Mass spectrometry

Mass spectrometry was performed on a Micromass Q-Tof Micro^{TM} (Waters MS Technologies, Manchester, UK) operating in positive and negative ion mode. The nebulization gas was set to 100 L/h for 1 mm separations and 300 L/h for 2.1 mm separations at a temperature of 250 °C. The cone gas was set to

0 L/h and the source temperature set to 120 °C. The capillary and cone voltages were set to 3200 and 30 V, respectively. The Q-Tof Micro was operated with a collision energy alternating between 5 and 25 eV. The data acquisition rate was set to 0.1 s, with a 0.1 s inter-scan delay. All analyses were acquired using the lock spray to ensure accuracy and reproducibility; leucine enkephalin was used as the lock mass (*m/z* 556.2771) at a concentration of 50 fmol/μL and flow rate 30 μL/min.

In the case of negative ESI the capillary voltage was set to 2400 V and a cone voltage of 40 V again with an alternating collision energy of 5 and 25 eV. Leucine enkephalin was employed as the lockspray at a concentration of 50 fmol/μL.

Data were collected in centroid mode, the lockspray frequency was set at 5 s, and data were averaged over 10 scans.

3.4. Data analysis for UPLC–MS

The raw data were analysed by the Micromass MarkerLynx applications manager Version 1.0 (Waters, UK); this application manager integrates peaks in the LC/MS data by using ApexTrack™ peak detection. The LC/MS data are peak-detected and noise-reduced in both the LC and MS domains such that only true analytical peaks are further processed by the software (e.g. noise spikes are rejected). A list of the intensities of the peaks detected is then generated for the first sample, using the retention time (RT) and *m/z* data pairs as the identifier for each peak. This process is repeated for each LC/MS run and the data from each LC/MS analysis in the batch are then sorted such that the correct peak intensity data for each RT–*m/z* pair is aligned in the final data table. The ion intensities for each peak detected are then normalized, within each sample, to the sum of the peak intensities in that sample. The resulting normalized peak intensities are then multiplied by 10,000 and the (RT–*m/z* pair) analysed by principal components analysis (PCA) using Pareto scaling. PCA analysis was carried out following the removal of the compound related ions for pravastatin itself and its glucuronide metabolite.

3.5. ^{1}H NMR spectroscopy

160 μL of neat urine were buffered with 80 μL 0.2 M phosphate buffer in D_2O (pH 7.4, to provide a field-frequency lock) containing TSP (sodium trimethyl-silylpropionic acid [$^2H_4$]), used as chemical shift reference ($\delta_{1H} = 0.0$) prior to analysis by NMR spectroscopy. Urinalysis was carried out on a Bruker DRX500 NMR spectrometer operating at 500 MHz ^{1}H resonance frequency, equipped with a 2.5 mm SEI NMR probe. ^{1}H NMR spectra were acquired at 30 °C, with 90 °C pulse widths over a spectral width of 9980.04 Hz into 64,000 data points. Typically, 256 transients were collected (as the urines were dilute as a consequence of continuous infusion) with an acquisition time of 3.28 s (and a relaxation delay of 2 s). Solvent suppression was achieved by applying the standard Noesypresat pulse sequence (Bruker Biospin Ltd.) with secondary irradiation of the dominant water signal during the mixing time of 150 ms and the relaxation delay of 2 s. No line broadening function was applied prior to FT.

3.6. Data analysis for ^{1}H NMR spectroscopy

All ^{1}H NMR spectra were manually corrected for phase and baseline distortions within XWINNMR™ (Version 2.6, Bruker Spectrospin Ltd.). Spectra were referenced to TSP (δ_{1H} 0.0) prior to data-reduction into 245 spectral integral regions corresponding to the chemical shift range of δ_{1H} 0.2–10 utilising AMIX (version 2.7.5, Analysis of MIXtures, Bruker Spectrospin Ltd.). The region of δ_{1H} 4.52–6.0 was set to zero to remove the effects of variations in the presaturation of the water resonance in all NMR spectra, and to alleviate cross-relaxation effects in the urea signal via solvent exchanging protons. Integration into bins (or buckets) across the spectral regions of 0.04 ppm was performed automatically in AMIX.

The integral values in each spectrum were then normalized, i.e. scaled, to the total intensity for that spectrum to compensate for differences in dilution between the samples. The resulting data matrix (peak integral values/bins per sample) was analysed by principal components analysis (PCA) using SIMCA-P (Version 10, UMETRICS AB, Box 7960, SE 90719, Umeå, Sweden). The resonances arising from pravastatin-related material were removed from the data prior to PCA analysis.

4. Results and discussion

4.1. Histopathology and clinical chemistry

Conventional clinical chemistry was performed on samples obtained from both the control and dosed animals. Markedly increased plasma enzyme values (Table 1) were observed for two of the dosed animals (numbers 3 and 4) and were generally considered to be consistent with liver toxicity. Visual examination of the livers for animals 3 and 4 showed them to be pale and discoloured. Histopathology of the liver showed that continuous infusion of 500 mg/kg/day of pravastatin for 4 days caused minimal hepatocyte necrosis in one animal (number 2) and more

Table 1
Effects of pravastatin on plasma enzymes and metabolites on day 4 of continuous intravenous administration at 500 mg/(kg day)

Animal	Alkaline phosphatase (IU/L)	Alanine aminotransferase (IU/L)	Aspartate aminotransferase (IU/L)	Glucose (mmol/L)	Cholesterol (mmol/L)	Triglycerides (mmol/L)
1	61	42	65	13.7	1.2	0.81
2	77	83	123	7.8	1	0.36
3	155	1339	2311	8.1	0.5	0.38
4	209	3167	3930	5.9	1	0.46

pronounced hepatocyte necrosis in two animals (numbers 3 and 4). Continuous infusion of 500 mg/kg/day of pravastatin for 4 days also markedly increased plasma levels of the liver-specific enzymes alanine aminotransferase and aspartate aminotransferase in animals 3 and 4 (Table 1). These data are consistent with pravastatin causing greater liver toxicity in animals 3 and 4 compared to animal 2. Liver toxicity has been reported for statins administered at high doses in the rat [23,27] and other preclinical species, including pravastatin in the cynomolgus monkey [28]. This is likely to occur through excessive pharmacology, as such changes are prevented by co-administration of mevalonate, the product of HMG-CoA reductase [23]. Administration of toxicological doses of pravastatin and other statins has been shown to cause elevations of plasma bile acids, which may be indicative of cholestasis [29].

Effects were also noted on plasma glucose, cholesterol and triglyceride concentrations in all of the dosed animals and were of comparable magnitude in all three (Table 1). The reduced cholesterol and triglyceride values compared to the control were probably, at least in part, related to a reduction in dietary intake as well as the likely effects of both liver toxicity and the pharmacology of pravastatin.

5. UPLC–MS

A typical total ion current chromatogram obtained using gradient RP-UPLC on a 1 mm i.d. column, of urine obtained from the control and a dosed animal (rat 3) for day 4 of the study is shown in Fig. 2 for positive ESI. These chromatograms reveal clear differences between the profiles for the control and the dosed animal. Under these conditions UPLC produced sharp chromatographic peaks with an average width of 5–7 s at the base, giving a theoretical peak capacity of ca. 360 resolved peaks for the separation obtained here. This compares with traditional HPLC where analysis based on 3.5 μm particles generally results in average peak widths of 15–20 s, using optimal mobile

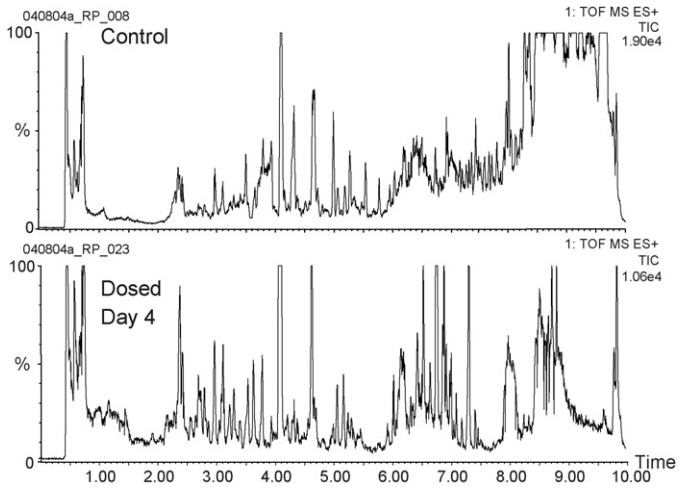

Fig. 2. A comparison of the UPLC–MS TICs obtained using the 1 mm i.d. column for the control (rat 1) and dosed (rat 3) animal on day 4 of pravastatin administration.

phase linear velocities, producing a peak capacity of 120. As the application of 1 mm i.d. columns has proved to be problematic in the past, due to some extent to the analytical instrument design (in particular the delay volume), the performance of the 1 mm i.d. column was compared to that of an equivalent 2.1 mm i.d. column. This comparison revealed that the microbore 1 mm i.d. columns provided significant advantages compared to the 2.1 mm i.d. columns in terms of increased sensitivity, reduced sample consumption and reduced chemical noise in the mass spectrometer as a result of the low flow rate. The extracted ion chromatograms for the $m/z = 255$ ion obtained for both 1 and 2.1 mm i.d. columns are displayed in Fig. 3. The peak width for both columns was determined to be 7 s at the base. There was a slight difference in retention time but this was essentially due to the delay volume in the instrument. The effect of column format on assay sensitivity was determined with the injection volume scaled to compensate for the differences in column diameter.

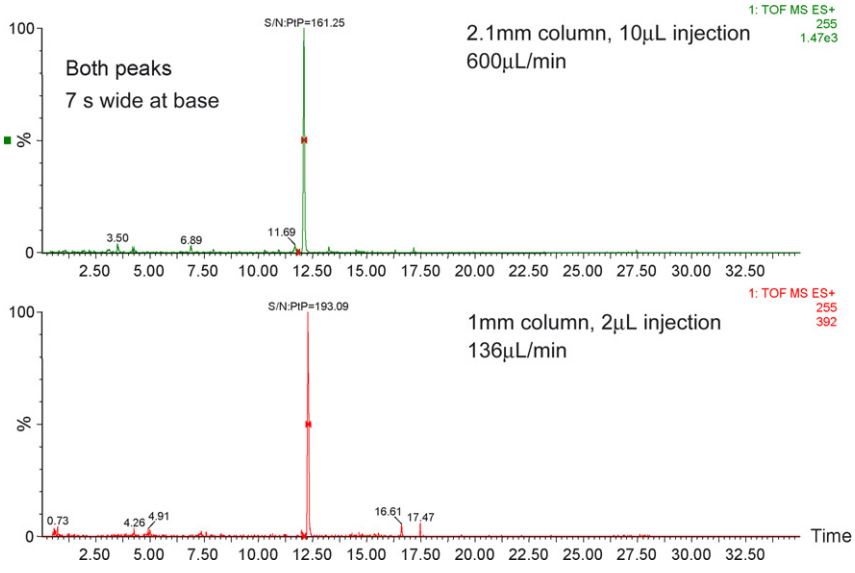

Fig. 3. A comparison of the chromatography obtained on 2.1 and 1 mm i.d. columns for the ion m/z 255 detected in the urine of one of the rats.

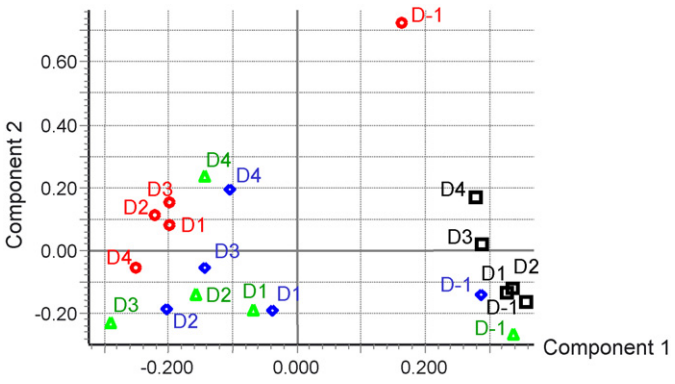

Fig. 4. PCA of the UPLC–MS data obtained over the 4 days of the study. Key: black squares, control animal (rat 1); red circles, rat 2; blue diamonds, rat 3; green triangles, rat 4. (For interpretation of the references to colour in this figure legend, the reader is referred to the web version of the article.)

Thus 2 μL was injected onto the 1 mm i.d. column and 10 μL onto the 2.1 mm i.d. column (the actual ratio should have been between 2 → 8.82) with a ca. 20% increase in signal-to-noise ratio, as a result of increased peak height, seen for the smaller diameter column (s/n 197:1 for the 1 mm and 161:1 for the 2.1 mm i.d. columns, respectively).

The UPLC/MS data generated on samples from the control and pravastatin-dosed animals were subjected to chemometric analysis (following the removal of the compound related ions for pravastatin itself and its glucuronide metabolite). The statistical analysis used employed mean centring of the data and Pareto scaling; the results of which are displayed in Fig. 4 for the positive ESI data. Thus the scores plot (Fig. 4) shows, as would be expected, that most of the day −1 samples from the control and dosed animals cluster closely together. However, on day −1 animal 2 appears to be a statistical outlier (although there was no evidence of this in the corresponding NMR spectrum), with the major ions responsible for the observed variation being *m/z* 242, eluting at 18.09 min, *m/z* 333 (17.4 min), *m/z* 349 (15.6 min) and *m/z* 412 (16.2 min). The identities of these components are unknown.

Whilst, following the commencement of pravastatin administration, the control animal remains in the "control" region of "metabolic space" for the rest of the study, this is not the case for the animals dosed with pravastatin as these rats move away from the control animal and their own pre-dose position. Two of the dosed animals (rats 3 and 4) progress through a metabolic trajectory, moving steadily away from the control position and reaching a maximum distance from the control/pre-dose samples on day 4 of the study. The remaining dosed animal (rat 2), which was the outlier on day −1 of the study also moved into a different metabolic space on dosing. However, for rat 2, a clear time-related trajectory was not observed. Based on the relative intensities of the pravastatin-related ions (prior to their removal for chemometric analysis) seen for the samples obtained for this animal it would appear that it had a lower exposure to the drug.

Whilst not readily detected in positive ESI pravastatin and its metabolites were easily detected in negative mode, and indeed dominated the dataset and confounded the interpretation of the data. Examination of the relative amounts of pravastatin-related material in the urine samples (data not shown) confirmed the much lower exposure to the drug of rat 2 compared with rats 3 and 4 (see also the NMR data below) and this may provide a partial explanation of the different metabolic response of rat 2 compared to the other animals.

The major ions contributing to the metabolic trajectory following dosing were, *m/z* = 279 at 13.5 min, *m/z* = 209.2 at 15.05 min, *m/z* = 233.21 at 15.05 min, and *m/z* = 183.18 eluting at 15.05 min, which were present in increased amounts in samples from the dosed (rats 3 and 4) compared to the control (rat 1). The data in Fig. 5 illustrates the relative response for the *m/z* = 279, 233 and 209 ions in animal 3 on day 2 of dosing compared to the control animal on the same day. These ions were present at low, almost undetectable, levels in the control samples, but rose on days 1 and 2 after the commencement of dosing (in all the dosed

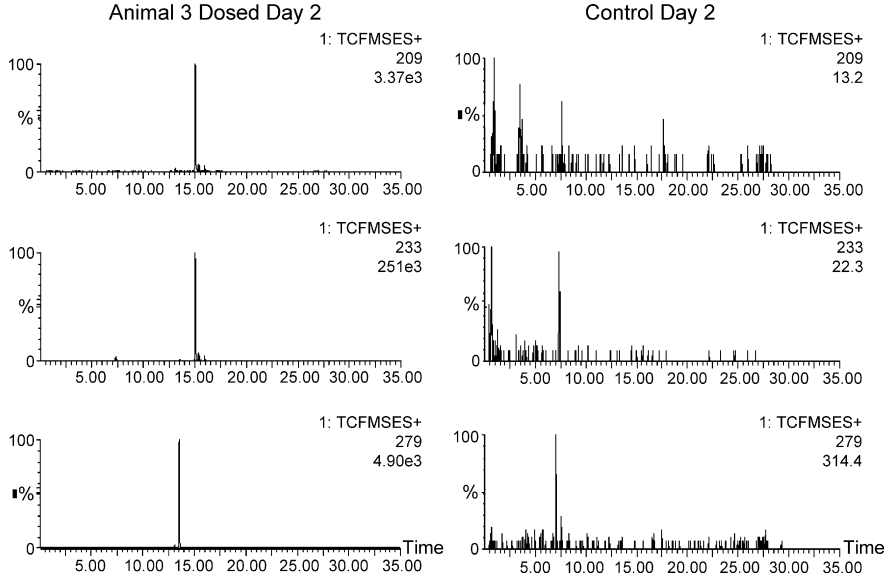

Fig. 5. The relative responses for the ions at *m/z* 209 (top), 233 (middle) and 279 (bottom) for a dosed animal (rat 3) and the control animal (rat 1).

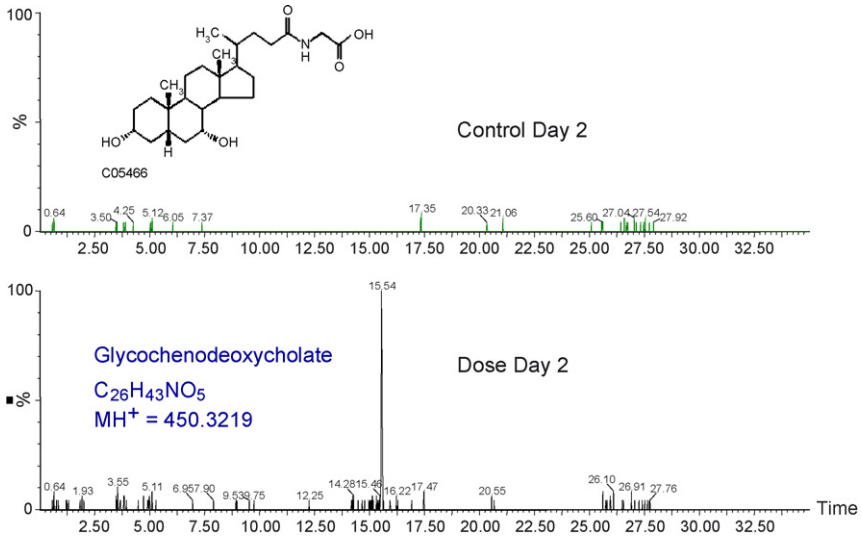

Fig. 6. The relative responses for a dosed animal (rat 3) and the control animal (rat 1) for the ion at *m/z* 450 corresponding to glycochenodeoxycholate for urine obtained for day 2 of dosing.

animals), before falling back on days 3 and 4 of the study. The ions responsible for the difference between the samples on days 3 and 4 were determined to be *m/z* = 357, eluting at 2.7 min, and *m/z* = 205, eluting at 5.50 min.

Another ion identified as contributing to the statistical result was the *m/z* = 450 ion eluting at 15 min. This analyte gave an exact mass value of 450.3212, which gives an elemental composition of $C_{26}H_{43}NO_5$ with a mass error of 1.6 ppm. A close inspection of the resulting MS spectrum for this compound, Fig. 6, and the co-elution with an authentic standard confirmed this analyte to be glycochenodeoxycholate, part of the bile acid biosynthesis pathway. Increases in bile acids have been reported as biomarkers in previous metabonomics studies examining hepatotoxicity using ^{1}H NMR spectroscopy [24]. In contrast to the animals 3 and 4, the concentrations of glycochenodeoxycholate remained close to pre-dose values in the control animal 1 and the dosed animal 2.

6. ^{1}H NMR spectroscopy

Visual examination of the NMR spectra clearly revealed that urine collected from animals treated with pravastatin differed from their pre-dose spectra and samples taken from animals receiving vehicle alone (Fig. 7). Post the commencement of dosing, resonances that could be assigned to pravastatin were observed in the urine of all of the dosed rats, with an increase in intensity occurring over time. However, drug-related material was not present at the same concentration in the urine of all three dosed animals with the resonances being more prominent in the samples obtained from animals 3 and 4 compared to that of animal 2. Concomitantly, marked perturbations to the endogenous urinary metabolite profile associated with exposure to pravastatin were observed for animals 3 and 4. Thus, decreases were observed in urinary hippurate concentrations on days 2, 3 and 4 post-dosing, and in citrate, α-ketoglutarate and succinate on days 3 and 4 (with citrate being reduced for animal 3 also on day 2). Furthermore, marked increases were observed in creatine on days 3 and 4 and taurine on day 2 (for animal 4) and days 3 and 4 (in animals 3 and 4). These changes were supported by the PCA-generated loadings plot of the NMR data (data not shown). Further changes in the NMR spectra of rats 3 and 4, although not highlighted in the loadings plot, included decreased concentrations of TMAO and slight reductions in acetate, DMG, allantoin and creatinine (based on the signal at 4.05 ppm), as these signals were either obscured by pravastatin-resonances and hence, omitted from PCA-analysis, or were overlapped with other signals, such as the case with taurine and TMAO (the taurine-triplet at 3.26 ppm increased, while the TMAO-signal at 3.27 ppm decreased in the same integral bucket). In addition, in the urine of both animals, an increase in bile acid-related signals was observed on day 4 (presumably glycochenodeoxycholate based on the UPLC–MS result).

In contrast, animal 2 showed no significant perturbation of the endogenous metabolite profile, which, based on the low intensities of the pravastatin signals observed in the urine, implies an apparent lower exposure to the drug (data not shown). Chemometric analysis (PCA) of the data set, with the pravastatin resonances removed prior to normalisation, clearly demonstrates the marked response observed for animals 3 and 4 compared to animal 2 whose data points cluster near to the pre-dose and control data in the scatter plot (Fig. 8). For animals 3 and 4, the time course of the response, with the perturbations being greatest on days 3 and 4 is also evident, and similar to that seen using UPLC–MS.

The perturbations in metabolite profiles described here are characteristic of hepatotoxicity and this general conclusion is supported by the results of both clinical chemistry and histopathology. Thus an ^{1}H NMR-based metabonomic study in rats on the hepatotoxin α-naphthylisothiocyanate observed increased urinary taurine and creatine and bile acids accompanied by decreased excretion of TCA cycle intermediates and hippurate [24,25]. Alterations to hippurate excretion have also been reported following changes to gut microflora, accompa-

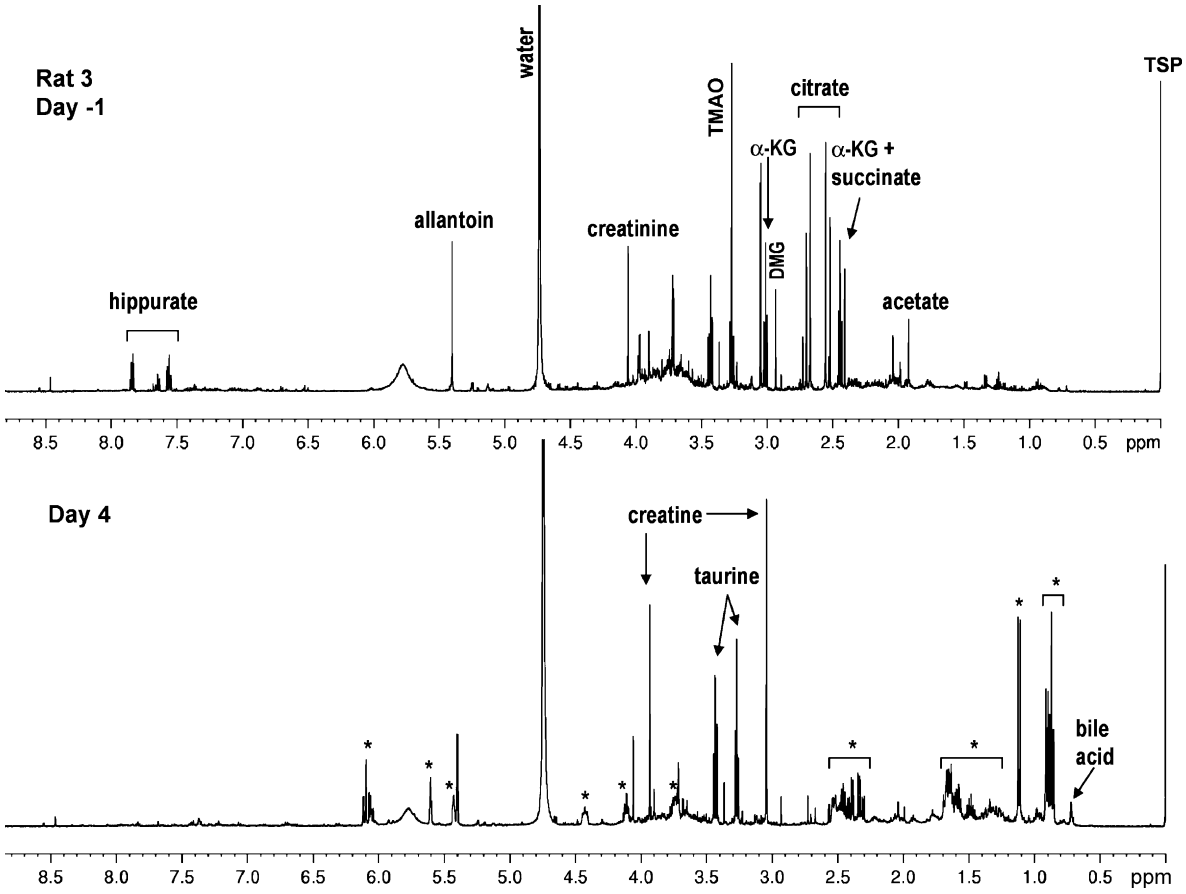

Fig. 7. ^{1}H NMR spectra of urine from a pravastatin-dosed animal (rat 3) for days 1 and 4 of the study. Key: *signals from pravastatin; α-KG, α-ketoglutarate; TSP, internal reference standard (sodium trimethyl-silylpropionic acid [$^{2}H_4$]).

nied by other changes in the aromatic excretion profile [26]. Of course where there is hepatic damage this may well be reflected in, e.g. reduced bile output, that might well have significant effects on the gut micro-environment leading to changes in benzoic acid production and metabolism by the microflora (the precursor to hippurate biosynthesis in liver and kidney).

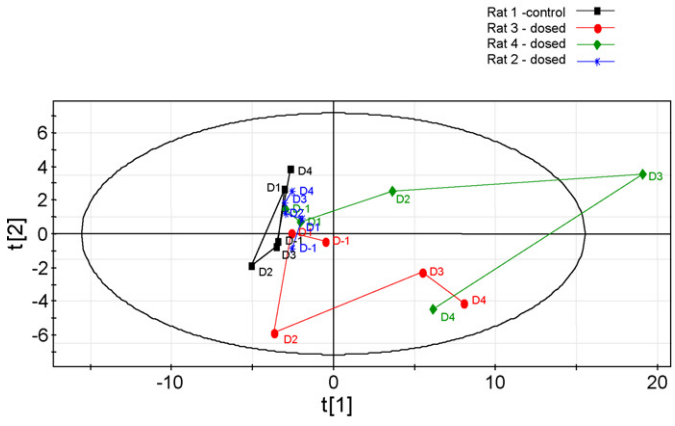

Fig. 8. NMR-PCA scatter plot $t[1]$ vs. $t[2]$ of data obtained from individual ^{1}H NMR spectra of urine collected from the control (rat 1) and the dosed animals (rats 2–4) on days −1, 1, 2, 3, and 4 of the study: the samples are connected over time to produce a trajectory for each animal. The resonances arising from pravastatin were removed from the data prior to PCA analysis. Key: black squares, rat 1; blue stars, rat 2; red circles, rat 3; green diamonds, rat 4. (For interpretation of the references to colour in this figure legend, the reader is referred to the web version of the article.)

Clearly the small numbers of animals used here does not permit robust statements to be made from the metabonomics data concerning the mechanism of the toxicological effects of pravastatin in this system. However, whilst it would obviously be unwise to over-interpret the data it is nevertheless possible to come to some general conclusions. Thus, despite the low number of animals used in this study we have successfully demonstrated the detection of biomarkers characteristic of hepatotoxicity using both ^{1}H NMR and UPLC–MS whilst providing at least a partial explanation for the absence of liver damage in one of the animals (rat 2). The reduced level of urinary pravastatin seen for animal 2 may reflect a dosing problem, with the animal having received a lower exposure to the drug, or it may reflect differences in the manner in which this particular animal handled the compound. Irrespective of the reason for the lower toxicity seen in rat 2, the fact that the pre-dose urine sample for this animal was seen to be significantly different, by UPLC–MS, from the others is very interesting. Arguably, had these pre-dose data been available before the commencement of the study this animal might have been replaced. Given the speed with which metabonomic analysis can be performed using both ^{1}H NMR and UPLC–MS this is not beyond the bounds of possibility and, had a "metabonomically" more normal animal been selected, the

result would possibly have been a more robust set of data. Indeed it would have been interesting, having collected urine samples pre-surgery, to see if this animal was metabolically normal or whether in fact it was already metabolically distinct. Despite the very small sample set it is also worth noting that the metabonomic data were entirely consistent with, and supportive of the results obtained from the clinical chemistry and histopathology data.

When performing animal experiments as part of drug discovery programs there is clearly a tension between the need to obtain robust data, which is often seen to require large numbers to counter variability, and the ethical and economic desire to use the minimum number of animals possible in order to make progress. In a study like the one described above, despite the fact that only a small number of animals formed the dataset, the combination of conventional and metabonomic techniques used did enable the liver to be identified as the primary site of toxicity, allowed the time course of the injury to be determined and allowed a major source of variability, in the response of animal 2, to be explained. It also provided some putative biomarkers for validation in further studies.

7. Conclusion

Thus, despite the small numbers of animals employed, the study was very information rich with concordant data from histopathological, clinical chemical and metabonomic analysis (using two platforms). This study therefore provides some confidence that first, the target organ for toxicity has been identified and secondly, that metabonomics could be used to monitor the onset and time course of this toxicity in subsequent studies, powered to generate a more robust statistical result.

References

[1] J.K. Nicholson, J.C. Lindon, E. Holmes, Xenobiotica 29 (1999) 1181–1189.
[2] J.K. Nicholson, J. Connelly, J.C. Lindon, E. Holmes, Nat. Rev. Drug Discov. 1 (2002) 253–258.
[3] J.C. Lindon, J.K. Nicholson, E. Holmes, in: D.G. Robertson, J.C. Lindon, J.K. Nicholson, E. Holmes (Eds.), Metabonomics in Toxicity Assessment, CRC Press, Boca Raton, 2005, pp. 105–172.
[4] J.C. Lindon, J.K. Nicholson, E. Holmes, H. Antti, M.E. Bollard, H. Keun, O. Beckonert, T.M. Ebbels, M.D. Reily, D. Robertson, G.J. Stevens, P. Luke, A.P. Breau, G.H. Cantor, R.H. Bible, U. Niederhauser, H. Senn, G. Schlotterbeck, U.G. Sidelmann, S.M. Laursen, A. Tymiak, B.D. Carr, L. Lehman-McKeeman, J.M. Colet, A. Loukaci, C. Thomas, Toxicol. Appl. Pharmacol. 187 (2003) 137–146.
[5] T.A. Clayton, J.C. Lindon, H. Antti, C. Charuel, G. Hanton, J.P. Provost, J.L. Le Net, D. Baker, R.J. Walley, J.E. Everett, J.K. Nicholson, Nature 440 (2006) 1073–1077.
[6] J.C. Lindon, E. Holmes, J.K. Nicholson, Prog. NMR Spectrosc. 45 (2004) 109–143.
[7] O. Fiehn, J. Kopka, R.N. Trethewey, L. Willmitzer, Anal. Chem. 72 (2000) 3573–3580.
[8] S. O'Hagan, W.B. Dunn, M. Brown, J.D. Knowles, D.B. Kell, Anal. Chem. 77 (2005) 290–303.
[9] R.A. Shellie, C.W. Welthagen, J. Zrostlikova, J. Spranger, M. Ristow, O. Fiehn, R. Zimmermann, J. Chromatogr. A 1086 (2005) 83–90.
[10] R.S. Plumb, C.L. Stumpf, M.V. Gorenstein, J.M. Castro-Perez, G.J. Dear, M. Anthony, B.C. Sweatman, S.C. Connor, J.N. Haselden, Rapid Commun. Mass Spectrom. 16 (2002) 1991–1996.
[11] A. Lafaye, C. Junot, B. Ramounet-le Gall, P. Fritsch, J.-C. Tabet, E. Ezan, Rapid Commun. Mass Spectrom. 17 (2003) 2541–2549.
[12] H. Idborg-Bjorkman, P.-O. Edlund, O.M. Kvalheim, I. Schuppe-Koistinen, S.P. Jacobsson, Anal. Chem. 75 (2003) 4784–4792.
[13] I.D. Wilson, J.K. Nicholson, J. Castro-Perez, J.H. Granger, K. Johnson, B.W. Smith, R.S. Plumb, J. Proteome Res. 4 (2005) 591–598.
[14] T. Soga, Y. Ohashi, Y. Ueno, H. Naraoka, M. Tomita, T. Nishioka, J. Proteome Res. 2 (2003) 488–494.
[15] L. Jia, S. Terabe, in: S. Vaidyanathan, G.G. Harrigan, R. Goodacre (Eds.), Metabolome Analysis, Springer, New York, 2005, pp. 83–101.
[16] E.M. Lenz, I.D. Wilson, J. Proteome Res. 6 (2007) 443–458.
[17] E.M. Lenz, J. Bright, R. Knight, I.D. Wilson, H. Major, Analyst 129 (2004) 535–541.
[18] E.M. Lenz, J. Bright, R. Knight, I.D. Wilson, H. Major, J. Pharm. Biomed. Anal. 35 (2004) 599–608.
[19] E.M. Lenz, J. Bright, R. Knight, F.R. Westwood, D. Davies, H. Major, I.D. Wilson, Biomarkers 10 (2005) 173–187.
[20] R.E. Williams, E.M. Lenz, A.J. Wilson, J. Granger, I.D. Wilson, H. Major, C. Stumpf, R. Plumb, Mol. Biosyst. 2 (2006) 174–183.
[21] R.S. Plumb, J.H. Granger, C.L. Stumpf, K. Johnson, B.W. Smith, S. Gaulitz, I.D. Wilson, J. Castro-Perez, Analyst 130 (2005) 844–849.
[22] R.S. Plumb, K.A. Johnson, P. Rainville, B.W. Smith, I.D. Wilson, J.M. Castro-Perez, J.K. Nicholson, Rapid Commun. Mass Spectrom. 20 (2006) 1989–1994.
[23] R.J. Gerson, J.S. McDonald, A.W. Albert, D.J. Kornburst, J.A. Majka, R.J. Stubbs, D.L. Bokelman, Am. J. Med. 87 (1989) 28S–38S.
[24] B.M. Beckwith-Hall, J.K. Nicholson, A.W. Nicholls, P.J. Foxall, J.C. Lindon, S.C. Connor, M. Abdi, J. Connelly, E. Holmes, Chem. Res. Toxicol. 11 (1998) 260–272.
[25] N.J. Waters, E. Holmes, A. William, C.J. Waterfield, R.D. Farrant, J.K. Nicholson, Chem. Res. Toxicol. 14 (2001) 1401–1412.
[26] A.N. Phipps, J. Stewart, B. Wright, I.D. Wilson, Xenobiotica 28 (1998) 527–537.
[27] J.S. MacDonald, R.J. Gerson, D.J. Kornbrust, M.W. Kloss, S. Prahalada, P.H. Berry, A.W. Alberts, D.L. Bokelman, Am. J. Cardiol. 62 (1988) 16J–27J.
[28] S. Sudo, K. Yamashita, N. Miyakoshi, N. Matsunuma, H. Tanase, H. Masuda, S.J. Manabe, Toxicol. Sci. 14 (1989) 57–83.
[29] P.F. Smith, R.S. Eydelloth, S.J. Grossman, R.J. Stubbs, M.S. Schwartz, J.I. Germershausen, K.P. Vyas, P.H. Kari, J.S. MacDonald, J. Pharmacol. Exp. Ther. 257 (1991) 1225–1235.